Adaptive-TTCM-Aided Near-Instantaneously Adaptive Dynamic Network Coding for Cooperative Cognitive Radio Networks

Wei Liang, Hung Viet Nguyen, Soon Xin Ng, *Senior Member, IEEE*, and Lajos Hanzo, *Fellow, IEEE*

***Abstract*—An adaptive dynamic network coding (ADNC) scheme conceived for cooperative cognitive radio (CCR) is proposed for devising a novel ADNC-CCR system. The system is designed for supporting communications between multiple primary users (PUs) and a common base station (BS), where the independent source information is transmitted from the PUs to the BS with the aid of multiple cognitive users (CUs) acting as relay nodes (RNs). To facilitate the recovery of the source information at the BS, the CUs invoke the ADNC technique, which is assisted by our cooperative protocol operating by exchanging the CCR-based control information between near-instantaneously adaptive turbo trellis coded modulation (ATTCM) and network coding (NC) codec, as well as between the CUs and the BS. More particularly, near-instantaneous ATTCM is employed for appropriately adjusting both the modulation mode and the code rate of the channel coding itself and of the NC, according to the near-instantaneous channel conditions. As a result, our novel ADNC-CCR system constructed on the basis of our holistic approach is capable of providing an increased throughput, despite reducing the transmission period of the PU. This reduced transmission period can also be directly translated into an increased duration for secondary communications of the CUs. In our proposed ADNC-CCR scheme, both the PUs and CUs employ our ATTCM scheme. As an additional novelty, the network encoder may also be activated in its adaptive mode for supporting the CUs, depending on the Boolean value of the feedback flags generated based on the success/failure of the ATTCM decoder and of the network decoder, which is evaluated and fed back by the BS. Quantitatively, it was found that the joint holistic design of our ATTCM-ADNC-CCR scheme is either capable of freeing up an approximately 40% of the PU's bandwidth in comparison to its noncooperative counterpart or increasing the attainable throughput by 2 bits/symbol.**

***Index Terms*—Adaptive turbo trellis coded modulation (ATTCM), cognitive radio network, cooperative communication, dynamic network coding.**

Manuscript received October 17, 2014; revised February 9, 2015; accepted March 5, 2015. Date of publication March 11, 2015; date of current version March 10, 2016. This work was supported in part by the European Research Council under an Advanced Fellow Grant, by the India–U.K. Advanced Technology Centre, and by the European Union's Seventh Framework Program (FP7/2007-2013) through the CONCERTO Project under Grant 288502. The review of this paper was coordinated by Prof. M. Uysal.

W. Lang, S. X. Ng, and L. Hanzo are with the Southampton Wireless Group, School of Electronics and Computer Science, University of Southampton, Southampton SO17 1BJ, U.K. (e-mail: wl7g09@ecs.soton.ac.uk; sxn@ecs.soton.ac.uk; lh@ecs.soton.ac.uk).

H. V. Nguyen is with the Post and Telecommunications Institute of Technology, Hanoi 10000, Vietnam, and also with the Southampton Wireless Group, School of Electronics and Computer Science, University of Southampton, Southampton SO17 1BJ, U.K. (e-mail: hvn08r@ecs.soton.ac.uk).

Color versions of one or more of the figures in this paper are available online at http://ieeexplore.ieee.org.

Digital Object Identifier 10.1109/TVT.2015.2412039

I. Introduction

THE POPULAR cognitive radio (CR) mechanism is capable of exploiting the temporarily available spectrum holes in the frequency domain. If a spectral slot is not used by the primary users (PUs), then the cognitive users (CUs) (or secondary users) would gain an opportunity to access it for their secondary communications based on the CR technique [1]–[3]. Spectrum allocation and sharing techniques have been widely investigated, to exploit the spectral bands more efficiently and to provide mutual benefits for the PUs and CUs [4]. However, both the availability and quality of a released spectral band is crucially influenced by both the specific activity and the competition between the PUs and CUs [4]. In this context, the most common paradigms in spectrum allocation and sharing are the underlay, overlay, and interwave schemes [5]. In the underlay scheme, the CUs are allowed to transmit their data simultaneously with PUs, provided that the interference imposed remains below the tolerate limit. In contrast to the underlay scheme, the interference imposed on the PUs under the overlay scheme may be offset by using part of the CU's power to relay the PU's information. Finally, in the interwave scheme, the CUs avoid simultaneous transmissions with the PUs [5].

Cooperative communication constitutes a novel paradigm that promises significant improvements by providing either an improved integrity or an increased throughput with the advent of user cooperation [6], [7]. Hence, in recent years, numerous exciting new applications of relay-aided communications have emerged [8]. More specifically, we have investigated the applications of relay-aided communications that may involve not only the physical layer [9] but also the medium access control layer [10] and the network layer, as well as their cross-layer operation [11]. One of the emerging applications is based on supporting communications between the source and destination nodes with the aid of cooperative protocols. A sophisticated medium access protocol was designed in [10], [12] for communications between the source and relay nodes (RNs), which relied on efficient modulation and coding [13], [14]. Moreover, in network-coding-aided systems designed for multiuser operation, the users can also act as cooperating partners or relays to share their resources and to assist each other in their information transmission [15]–[18]. The performance of CR schemes relying on one-way relaying was documented in [19] and two-way relaying in [20]. We found that 40% bandwidth reduction of PUs can be achieved by user cooperation.

Network coding (NC), which was proposed by Ahlswede *et al.* in 2000 [21], is capable of beneficially increasing the network capacity by invoking coding at the nodes of a network, in contrast to simply supporting routing functions. According to Yeung [22]: "NC has propagated to various fields in engineering in the past decade, including wireless communications, channel coding, computer networks, switching theory, cryptography, computer networks, data storage and computer science." Moreover, NC has been shown to be capable of increasing the achievable throughput, robustness, and security, while minimizing both the amount of dissipated energy and the delay of packets traveling through the network [21], [23]. The benefits of NC-aided cooperative systems were studied in [24]–[26] with the most important one being the reduction of redundant information transmissions [26].

Dynamic network codes (DNCs) were proposed in [15], where each user broadcasts its own information frames both to the base station (BS) and to the other users during the first transmission period. After this phase, each user transmits a nonbinary linear combination of its own frames and of the other users' information frames, to the BS [15]. The family of generalized DNCs (GDNCs) [16], [17] constitutes an extension of DNCs. In contrast to [15], in the proposal of [17], each user is allowed to broadcast several information frames during the broadcast phase via orthogonal channels [17] and to transmit several nonbinary linear combinations as parity frames during the cooperative phase via orthogonal channels. To increase the average transmission rate of GDNC without reducing its diversity order, in [16], an adaptive network code design has been proposed. The design of network codes for multiuser multirelay scenarios has been investigated in [18] and [27], where the users transmit their independent information to the BS with the aid of the RNs. In line with the system model proposed in [18], we assume that the CUs act as the RNs to help the PUs in transmitting their information to the BS. More specifically, in our proposed scheme, the CUs are capable of relaying the PU's message, while superimposing their own messages at the same time. This leads both to an increased overall throughput and to the reduction of the required transmission period of both the PUs and the CUs, thereby creating additional time slots (TSs) for supporting additional users.

In this paper, we consider cooperation between the PUs and CUs, where the CUs may act as NC-aided RNs for the sake of conveying information transmitted from the PUs. Our contributions in [19] and [20] only considered simple RNs without the capability of invoking NC. More explicitly, the NC schemes of [15]–[18] were intrinsically amalgamated with an active-cooperation-based overlay network conceived for a CR system. In contrast to [28], we considered intelligent CUs that are capable of employing NC techniques for their data transmission. Additionally, we invoked adaptive DNC (ADNC) [16], where the CUs deliver their information to the BS, only if the BS failed to recover the source messages from the PUs. Additionally, our proposed ADNC-aided cooperative CR (CCR) scheme is intrinsically amalgamated with near-instantaneously adaptive coded modulation. Explicitly, we have opted for using bandwidth-efficient turbo trellis coded modulation (TTCM) [29], [30], because it was shown to outperform trellis coded modulation (TCM), bit-interleaved coded modulation (BICM), and iteratively decoded BICM [29].

Based on this background, the novel contribution of this paper is that a realistic adaptive TTCM (ATTCM) arrangement is designed for conceiving an ADNC-CCR system to simultaneously improve both the system's throughput and its resilience. More specifically, the contributions of this paper are as follows.

1) An active cooperation-aided DNC scheme was proposed for overlay based CCR schemes to lease the PU's bandwidth to the group of CUs for their secondary communication.
2) A bandwidth-efficient ATTCM arrangement is conceived for our proposed scheme for achieving a substantial performance improvement. The transmission rate/throughput of the system is adapted according to the near-instantaneous channel conditions, where a higher throughput but vulnerable TTCM scheme is employed when the channel conditions are good, whereas a lower throughput but robust TTCM scheme or no transmission is used, when the near-instantaneous channel conditions are poor. Specifically, our ATTCM scheme is designed by considering the effects of both quasi-static Rayleigh fading and of uncorrelated Rayleigh fading.
3) Moreover, as prophesied in [16], we have conceived an ADNC technique for our novel CCR system, where the CUs adaptively deliver their parity frames to the BS, depending on the success/failure of the PU's transmissions. Our proposed ADNC-CCR scheme relies on a cutting-edge channel coding scheme, which increases the achievable multiplexing gain, despite imposing low complexity.
4) In our proposed system, each transmission link employs different ATTCM modes. During each broadcast session, all PUs transmit using the same fixed TTCM mode, which corresponds to that determined by the specific direct link having the lowest quality. Then, in the cooperative phase, the "best" CU would support all the transmissions toward the BS with the aid of its highest throughput ATTCM mode. The received SNRs at the CUs and the BS may be used for determining the maximum throughput of each transmission link.
5) Finally, we conceived a novel ATTCM-aided ADNC scheme for overlay CCR systems, which is capable of simultaneously exploiting the advantages of ATTCM and ADNC for facilitating a further improvement of our system's performance.

This paper is organized as follows. Section II presents our system model and outlines the NC scheme, the ATTCM scheme, and the ADNC. Our novel ATTCM-ADNC-CCR arrangement is described in Section III. The performance of our proposed scheme is evaluated in Section IV. Finally, our conclusions are presented in Section V.

II. System Model

In our proposed system shown in Fig. 1, we consider the uplink (UL) transmission of the ADNC-CCR network. ATTCM

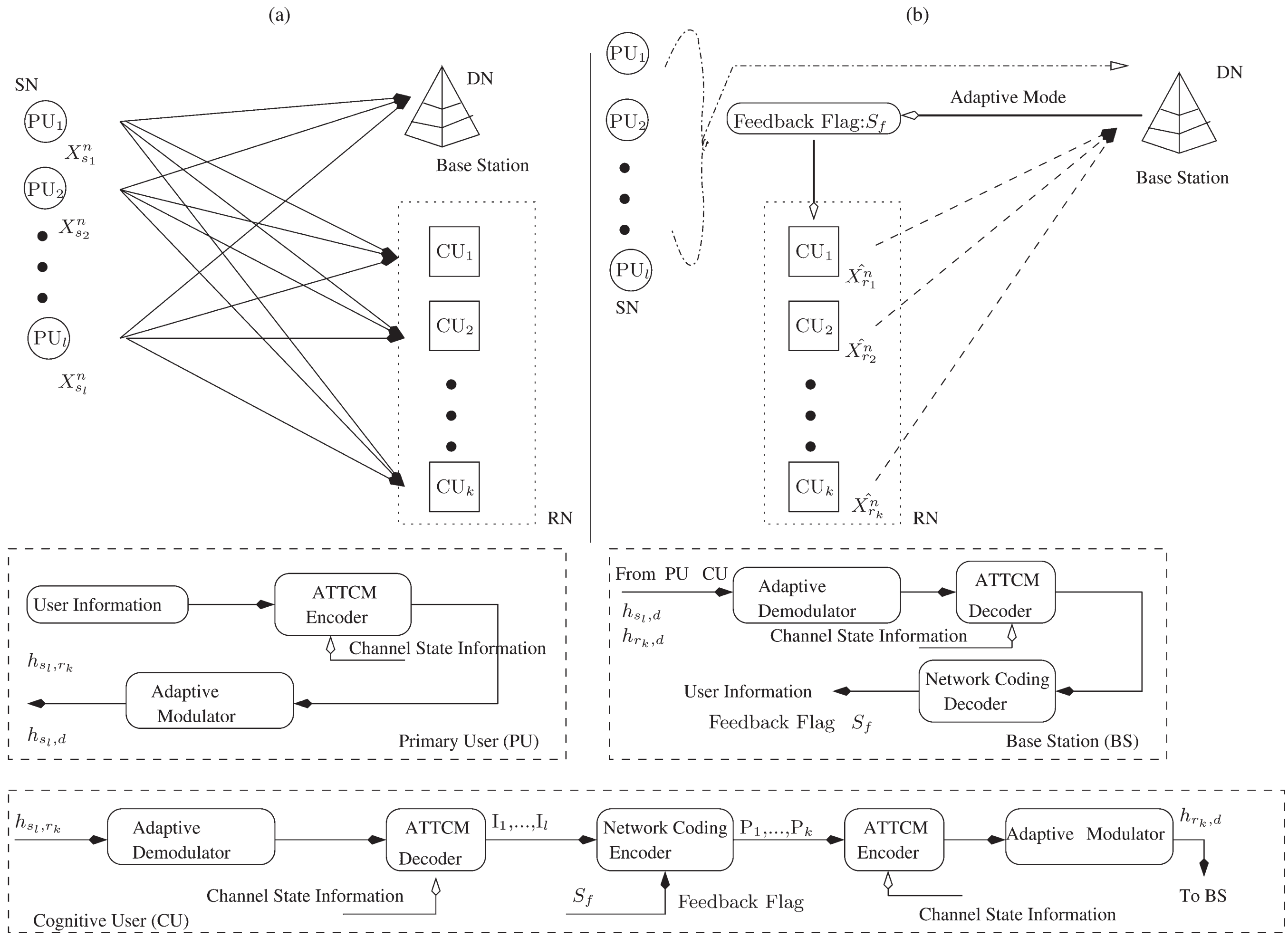

Fig. 1. Architecture of the ATTCM-aided DNC in the proposed CCR scheme. (a) Broadcast phase. (b) Cooperative phase.

is advocated for judiciously selecting a suitable modulation mode according to the near-instantaneous channel condition experienced in each transmission link, which would lead to the reduction of the PU's transmission power and/or to the increase in the overall system throughput, hence simultaneously saving bandwidth for the CUs. We assume that each PU has a direct transmission link to the BS, as shown in Fig. 1. In addition, we consider L PUs, where each PU broadcasts its information to a single BS and to K CUs during the broadcast phase. The BS then decodes the source information received from the PUs. Accordingly, the CUs encode the received information frames for constructing the corresponding parity frames, which are then transmitted to the BS during the cooperative phase. Hence, the BS receives the information frames from the PUs and the parity frames from the CUs.

During the "broadcast phase" shown in Fig. 1, the lth PU/SN broadcasts its information frame $X_{s_l}^n$ within the nth frame to both the CUs/RNs and to the BS. The signal received at the BS via the source-to-destination (SD) link is given by

$$y_{s_l d}^n = \sqrt{G_{s_l d}}\sqrt{P_S} h_{s_l d} X_{s_l}^n + n \tag{1}$$

whereas that received at the k CU/RN via the source-to-relay (SR) link is

$$y_{s_l r_k}^n = \sqrt{G_{s_l r_k}}\sqrt{P_S} h_{s_l r_k} X_{s_l}^n + n \tag{2}$$

where P_S is the transmission power per unit frequency emanating from the PU/SN and $n \in N$, where N is the total number of frames. The $(N \times L)$ PUs simultaneously broadcast $(N \times L)$ information frames during the time duration T_1. Since an NC-aided decode-and-forward protocol is employed at each CU/RN, the kth RNs forward the decoded and reencoded information frame $\hat{X_{r_k}^n}$ during the nth frame to the BS. Then, during the "cooperative phase" of Fig. 1, the signal received at the BS via the relay-to-destination (RD) link can be formulated as

$$y_{r_k d}^n = \sqrt{G_{r_k d}}\sqrt{P_{\mathrm{CU}}} h_{r_k d} \hat{X_{r_k}^n} + n \tag{3}$$

where the CU/RN forwards the source information frame using the power P_{CU}. Similar to the broadcast phase, the overall transmissions during the cooperative phase are within the time duration of T_2. In our proposed system, the CUs act as the RNs, where the RNs are located halfway between the PUs and the BS. Accordingly, the reduced-distance-related path-loss reduction (RDRPR) [31], [32] experienced by the SR link is given by

$$G_{\mathrm{sr}} = \left(\frac{d_{\mathrm{sd}}}{d_{\mathrm{sr}}}\right)^{\alpha} \tag{4}$$

where α is the path-loss exponent [33]. Similarly, the RDRPR of the RD link with respect to the SD link is given by

$$G_{\mathrm{rd}} = \left(\frac{d_{\mathrm{sd}}}{d_{\mathrm{rd}}}\right)^{\alpha}. \tag{5}$$

Naturally, the RDRPR of the SD link with respect to itself is unity, i.e., we have $G_{s_l d} = 1$. We consider an outdoor environment [33], where $\alpha = 3$. Note that the same RDRPR is exploited by all the SR and RD links in our system. Thus, we have $G_{s_l r_k} = G_{r_k d} = 2^3 = 8$. Moreover, we consider a single nondispersive transmission path for the SD, SR, and RD links of our novel ATTCM-ADNC-CCR scheme. Each of the channels in (1)–(3) is comprised of two components, which may be expressed as

$$h = h_s \cdot h_f \tag{6}$$

where the slow fading (or quasi-static fading) coefficient h_s is constant for all symbols within a transmit frame. By contrast, the fast-fading (small-scale Rayleigh fading) coefficient h_f varies on a symbol-by-symbol basis, which will be described in Section II-A. According to (1)–(3), the average received SNR at node b per frame is given by

$$\begin{aligned}\gamma_R &= \frac{G_{ab} E\left[|x|^2\right] E\left[\left|h_f^2\right|\right] E\left[\left|h_s^2\right|\right]}{N_0} \\ &= \frac{G_{ab}|h_{ab}|^2}{N_0}\end{aligned} \tag{7}$$

where we have $E[|x|^2] = 1$ and $E[|h_f^2|] = 1$ for uncorrelated Rayleigh fading channels, which varies on a symbol by symbol basis, as discussed in Section II-A, and we have $E[|h_s^2|] = |h_s|^2 = |h_{ab}|^2$. Then, we determine the received SNRs of the $[l(k+1)+k]$th communication links by referring to Fig. 1, which are $[\gamma_{s_l d},\ \gamma_{s_l r_k},\ \gamma_{r_k d}]$.

A. Adaptive TTCM

Employing ATTCM has the advantage that the system's effective throughput can be increased upon increasing the code rate and constellation size when the channel quality improves, which is achieved without any bandwidth expansion. Furthermore, the bit error ratio (BER) and frame error ratio (FER) performance of the system may be improved [34]. In Fig. 1, both the PUs and CUs have employed ATTCM encoders, where the TTCM encoder comprises a pair of identical parallel-concatenated TCM encoders [35] linked by a symbol interleaver. The first TCM encoder directly processes the original input bit sequence, whereas the second one encodes the interleaved or scrambled version of the input bit sequence. Then, the bit-to-symbol mapper maps the input bits to complex-valued ATTCM symbols using the classic set-partition-based labeling method [34]. Additionally, the BS decodes the information delivered from the PUs and CUs by the ATTCM decoder. The structure of the TTCM decoder is similar to that of binary turbo codes, where each decoder alternately processes its corresponding encoder's channel-impaired output symbol and then the other encoder's channel-impaired output symbol [34, pp. 764]. As shown in Fig. 1, we invoked a near-instantaneously ATTCM scheme for protecting the SR and the RD links, where the effective throughput range is given by $R_{\mathrm{tran}} = \{0, 1, 2, 3, 4, 5\}$ bits per symbol (BPS), when no transmission, quadrature phase-shift keying (PSK), 8PSK, 16-ary quadrature amplitude modulation (16QAM), 32QAM, and 64QAM are considered, respectively.

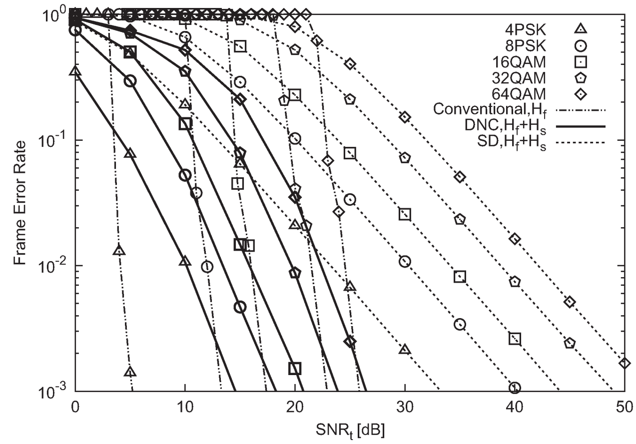

Fig. 2. FER performance versus SNR$_t$ of TTCM for five fixed modulation modes. "Conventional" represents the FER performance of TTCM using a frame length of 12 000 symbols when communicating over Rayleigh fading channels. Four TTCM iterations were invoked. "DNC" and "SD" denote the FER performance of TTCM-DNC and TTCM-aided noncooperative schemes for five fixed modulation modes using 10^6 frames when communicating over the combined uncorrelated Rayleigh fading and quasi-static fading channels.

Moreover, the ATTCM mode switching thresholds $\Upsilon = [\gamma_0, \gamma_1, \gamma_2, \gamma_3, \gamma_4]$ were determined based on the FER performance curves of each of the five TTCM schemes when communicating over a Rayleigh fading channel, which is shown in Fig. 2. Specifically, both the ATTCM mode switching operation and the transmission rate of the modes are based on the following algorithm:

$$\mathrm{MODE} = \begin{cases} \gamma_4 \le \gamma_R, & \mathrm{TTCM} - 64\mathrm{QAM}, C^{*}{=}5 \text{ iBPS} \\ \gamma_3 \le \gamma_R < \gamma_4, & \mathrm{TTCM} - 32\mathrm{QAM}, C^{*}{=}4 \text{ iBPS} \\ \gamma_2 \le \gamma_R < \gamma_3, & \mathrm{TTCM} - 16\mathrm{QAM}, C^{*}{=}3 \text{ iBPS} \\ \gamma_1 \le \gamma_R < \gamma_2, & \mathrm{TTCM} - 8\mathrm{PSK}, C^{*}{=}2 \text{ iBPS} \\ \gamma_0 \le \gamma_R < \gamma_1, & \mathrm{TTCM} - 4\mathrm{PSK}, C^{*}{=}1 \text{ iBPS} \end{cases} \tag{8}$$

where C^* is the effective throughput in terms of the number of information bit per symbol (iBPS). Furthermore, we have considered two cases, when we have $\gamma_R < \gamma_0$ for the ATTCM mode switching operation. In the first case (case 1), no transmission is invoked to save energy when $\gamma_R < \gamma_0$. By contrast, the second case (case 2) invokes the 4PSK modulation mode

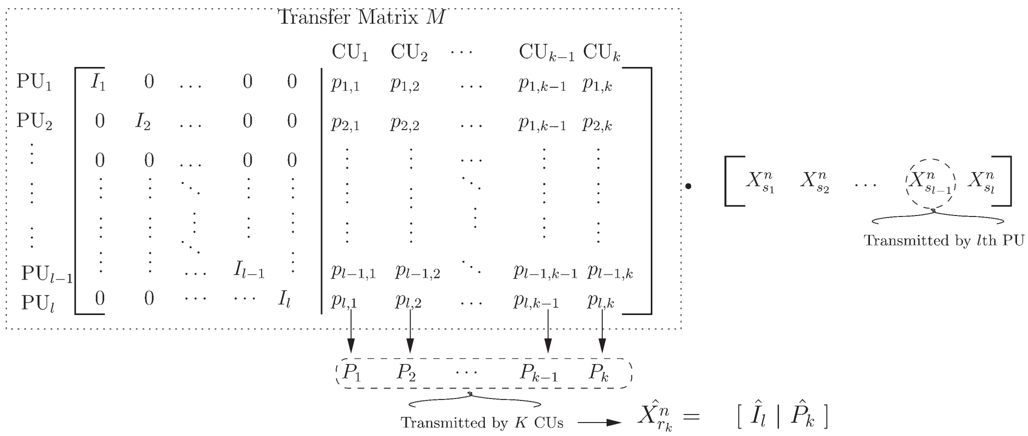

Fig. 3. Transfer matrix and the network encoding process engaged in the DNC-CCR scheme.

when $\gamma_R < \gamma_0$. Thus, the output C^* of these two cases may be expressed as

$$C^*(\gamma_R < \gamma_0) = \begin{cases} 0, & \text{case 1: No transmission} \\ 1, & \text{case 2: TTCM-4PSK.} \end{cases} \tag{9}$$

As shown in Fig. 2, we chose the switching thresholds carefully to ensure that the FER at the RN is lower than 10^{-3} to minimize the potential error propagation from the CUs to the BS, which are given by $\Upsilon_{\mathrm{ATTCM}} = [5.22, 12.25, 16.10, 21.15, 24.49]$ dB.

B. Network Encoder and Decoder

Here, the details on the encoding/decoding process of the NC technique are given. Fig. 1 shows how the CUs would successfully deliver the decoded information frames by employing the network encoding technique at the BS. The output codewords of the CUs are denoted as $\{\overleftrightarrow{\hat{X}^n_{r_k}}\}^K_{k=1}$, whereas those of the kth CU during the nth frame may be expressed as

$$\hat{X}^n_{r_k} = M \cdot X^n_{s_l} = [\hat{I}_l \mid \hat{P}_k] \tag{10}$$

where $X^n_{s_l}$ is the information frame transmitted from the lth PU within the nth frame to both the CUs and to the BS. Additionally, the transfer matrix M defined in [15] describes the corresponding network codes invoked for our DNC-CCR scheme. As shown in Fig. 3, the transfer matrix M is comprised of two components since we have $M = [I_l | P_k]$, where the identity matrix $\{I\}_l$ $(l \in L)$ represents the sequences transmitted from the PUs during the broadcast phase, whereas the parity matrix $\{P\}_{l\times k}$ $(k \in K)$ represents to the CUs' transmissions during the cooperative phase. Therefore, the corresponding entry I_l in Fig. 3 represents the successful/unsuccessful reception of the information frame recovered at the BS during the broadcast phase, which obeys the following rule:

$$I_l = \begin{cases} 0, & \text{if } X^n_{s_1} \text{ is not recovered successfully} \\ 1, & \text{if } X^n_{s_1} \text{ is recovered successful.} \end{cases} \tag{11}$$

We note that the coefficient $p_{l,k}$ shown in Fig. 3 is gleaned from the transfer matrix of a linear block code defined over the Galois field GF($|q|$), where $|q|$ is the alphabet size ($q = 2^b$), and b is an integer higher than zero [16], [18]. The transfer matrix constructed over the GF($|q|$) is provided by the software application SAGE [36]. As shown in Fig. 3, the variable $p_{l,k}$ represents the specific transmission state, during which the information frame is transmitted from PU_l to CU_k, as detailed in the following:

$$p_{l,k} = \begin{cases} 0, & \text{unsuccessful} \\ 1, & \text{successful.} \end{cases} \tag{12}$$

The network encoding process is represented by (10), where we construct the parity frames $\hat{P}_k = [P_1, P_2, \ldots, P_{k-1}, P_k]$ from the K CUs. Additionally, the parity frame transmitted by the kth CU is given by

$$P_k = I_1 p_{1,k} \oplus I_2 p_{2,k} \oplus \cdots \oplus I_l p_{l,k}. \tag{13}$$

As an illustration, we present a specific example associated with $L = 2$ PUs and $K = 2$ CUs, where we have orthogonal channels among the pairs of PUs and CUs, as shown in Fig. 4. We assumed that each PU broadcasts $m_1 = 1$ information frame, and then each CU transmits $m_2 = 1$ parity frame composed of the nonbinary linear combinations of its information frames defined over GF($|q|$) to the BS. Then, there are $(m_1 \times L + m_2 \times K) = 4$ phases during a transmission session, including the pair of broadcast phases BP_1 and BP_2 and the pair of cooperative phases CP_1 and CP_2. The coding

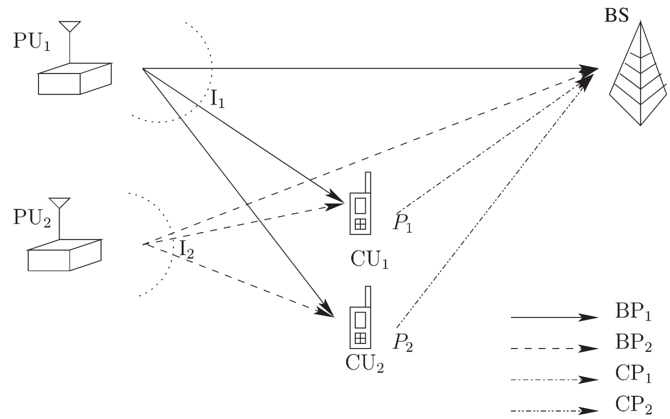

Fig. 4. Schematic of the DNC-CCR-scheme-based $M_{2\times 4}$ matrix. Two PUs intended to transmit their source messages I_1 and I_2, respectively.

arrangement of this specific example can be summarized as follows:

$$(\mathrm{BP}_1): \mathrm{PU}_1 \xrightarrow[(=0/1)]{I_1} \mathrm{CU}_1, \mathrm{PU}_1 \xrightarrow[(=0/1)]{I_1} \mathrm{CU}_2, \times\, \mathrm{PU}_1 \xrightarrow[(=0/1)]{I_1} \mathrm{BS} \quad (14)$$

$$(\mathrm{BP}_2): \mathrm{PU}_2 \xrightarrow[(=0/1)]{I_2} \mathrm{CU}_1,\ \mathrm{PU}_2 \xrightarrow[(=0/1)]{I_2} \mathrm{CU}_2, \times\, \mathrm{PU}_2 \xrightarrow[(=0/1)]{I_2} \mathrm{BS} \quad (15)$$

$$(\mathrm{CP}_1): \mathrm{CU}_1 \xrightarrow[(=0/1)]{\overbrace{M_{2\times4}(1,3)\cdot I_1}^{\mathrm{PU}_1\to\mathrm{CU}_1} \oplus \overbrace{M_{2\times4}(2,3)\cdot I_2}^{\mathrm{PU}_2\to\mathrm{CU}_1}} \mathrm{BS} \quad (16)$$

$$(\mathrm{CP}_2): \mathrm{CU}_2 \xrightarrow[(=0/1)]{\overbrace{M_{2\times4}(1,4)\cdot I_1}^{\mathrm{PU}_1\to\mathrm{CU}_2} \oplus \overbrace{M_{2\times4}(2,4)\cdot I_2}^{\mathrm{PU}_2\to\mathrm{CU}_2}} \mathrm{BS}. \quad (17)$$

Note that the arrow $\to$ represents the transmission direction. The notation 0/1 below the right arrow of (17) indicates whether the transmission was successful or not, where I_l is defined in (11) and $p_{l,k}$ in (12). The notation $\oplus$ represents the nonbinary linear combination of the information frames.

The corresponding transfer matrix $M_{2\times4}$ of [15] constructed for our specific system of Fig. 4 is defined as

$$M_{2\times4} = \begin{bmatrix} 1 & 0 & | & 1 & 1 \\ 0 & 1 & | & 1 & 2 \end{bmatrix} \quad (18)$$

where the subscript of $M_{N_r \times N_c}$ represents the matrix having N_r rows and N_c columns. Observe by referring to (13) that the parity frame is transmitted from CU_1 to the BS during CP_1 may be expressed as

$$P_1 = M_{2\times4}(1,3)I_1 \oplus M_{2\times4}(2,3)I_2 = I_1 \oplus I_2. \quad (19)$$

Then, the parity frame P_2 of from CU_2 during CP_2 becomes

$$P_2 = M_{2\times4}(1,4)I_1 \oplus M_{2\times4}(2,4)I_2 = I_1 \oplus 2I_2 \quad (20)$$

where $M_{2\times4}(i,j)$ represents row i and column j of the corresponding transfer matrix M, with $i \in [1,2]$ and $j \in [1,2,3,4]$.

We also define the modified transfer matrix $M'_{2\times4}$ with respect to the original transfer matrix $M_{2\times4}$, which takes into account the success/failure of each transmission during a specific transmission session. To detect the information frames of the PUs, the BS has to be aware of how each parity frame was constructed at the CUs. Hence, the modified transfer matrix $M'_{i\times j}$ is assumed known at the BS. If all the transmitted frames are successfully decoded, the modified transfer matrix is defined as $M'_{2\times4}(i,j) = M_{2\times4}(i,j)$. As shown in Fig. 1, $(K \times m_2)$ parity frames are transmitted by the K CUs, which contain the nonbinary linear combinations of its own information frames along with the successfully decoded information frames received from the L PUs. Let us denote the actual output codeword of the CUs as $\hat{X'}_{r_k{}^n}$ corresponding to the modified matrix $M'_{i\times j}$. Hence, $\hat{X'}_{r_k{}^n}$ contains all zeros, when the BS failed to successfully recover the $(L \times m_1)$ information frames or failed to receive the $(K \times m_2)$ parity frames; otherwise, we have $\hat{X'}_{r_k{}^n} = \hat{X}_{r_k{}^n}$.

C. Principle of Adaptive Dynamic Network Coding

In our ADNC scheme, we assume that the NC decoder at the BS is capable of sending back a feedback flag to the network encoders at the CU/RNs, as shown in Fig. 1. The transmission of the parity frames from the CUs is controlled by this feedback flag. In addition, we conceive and analyze an efficient ADNC scheme using two methods, namely M1 and M2, associated with different amounts of feedback requirements.

1) ADNC-M1: By referring to [16], the ADNC-M1 adaptively adjusts the number of frames transmitted from the CUs for each transmission session. The BS feeds back a single bit S_f, following the reception of a set of $(L \times m_1)$ information frames from the L PUs. If the CU/RNs received $S_f = 0$, this implies that the BS has failed to correctly decode the information frames received from all the PU/SNs; hence, the CU/RNs have to transmit $(K \times m_2)$ parity frames to the BS. Otherwise, if the BS successfully decoded the PU's information, the value of the feedback flag is set to $S_f = 1$. Let us denote the number of CUs invoked in an actual transmission by employing the ADNC technique during the cooperative phase as K'. The actual number of information frames $K'm_2$ transmitted from the K CUs by the ADNC-M1 technique obeys the following rules:

$$K'm_2 = \begin{cases} 0, & S_f = 1 \\ Km_2, & S_f = 0 \end{cases}$$

where m_2 denotes the number of information frame transmitted per CU.

2) ADNC-M2: In contrast to ADNC-M1, in the ADNC-M2 scheme, we assume that the BS feeds back L bits associated with the L PUs, namely S_{f_l}, to the CUs. Additionally, if the CUs received $\sum_{l=1}^{L}(S_{f_l}) = 0$, this implies that the BS has failed to correctly decode all the information packets received from the PUs; hence, the CUs have to transmit the same number of parity frames to the BS. Otherwise, the CUs do not have to transmit, provided that we have $\sum_{l=1}^{L}(S_{f_l}) = 1$, which indicates that the BS has indeed succeeded in flawlessly decoding all PUs' frames. Moreover, if most of the PUs' information frames are successfully received by the BS, except for the failed detection of ϑ PUs, then the CU may only have to transmit ϑm_2 number of parity frames to the BS. Hence, the number of parity frames required can be calculated by counting the specific number of the feedback flags indicating successful reception by the BS. More specifically, if the BS successfully received some of the information frames from the PUs, it will send a feedback flag to CUs, which will hence retransmit the failed information frames to the BS. Hence, the adaptive configuration of the actual number of K' CUs' information frames obeys the following rules:

$$K'm_2 = \begin{cases} 0, & \sum_{l}^{L}(S_{f_l}) = 1 \\ Km_2, & \sum_{l}^{L}(S_{f_1}) = 0 \\ \vartheta m_2, & \text{otherwise} \end{cases}$$

where ϑ denotes the number of CUs that have to relay the PU's information to the BS, i.e., $\vartheta \in L$. For example, the value of ϑ in our $M_{2\times 4}$-based scheme is 1, which implies that the BS failed to successfully decode a single PU's transmission. Additionally, in an $M_{N_r\times N_c}$-based scheme, the value of ϑ is given by $(K-i)$. The CUs would relay the required ϑ parity frames to the BS during the cooperative phase. The system's achievable performance will be discussed in Section IV.

III. System Design

Here, the design guidelines of our proposed system will be discussed first. Then, the transmission rates of both ADNC-M1 and ADNC-M2 are analyzed. Based on our investigations of both the NC rate and the diversity order of our ADNC-M1 and ADNC-M2 schemes, we decide upon our final recommended prototype system.

A. Adaptive TTCM Transmission Scenario

All transmission links shown in Fig. 1 have employed the ATTCM scheme detailed in (8) and (9), where each link may employ different modulation modes during the entire transmission period. Under the DNC policy of Section II-B, the PUs (or SNs) transmit at the same rate. We consider the "worst" PU, whose link toward both the CUs and the BS has the lowest SNR, which forces some of the PUs that actually experience a high SNR to transmit at a rate lower than their own affordable rate. This allows the CU to perform bit-by-bit combination of the decoded information. Thus, the lowest rate but most resilient modulation modes are activated for all the L SD links, which also affects the $(L\times K)$ SR links. The rate achievable at the SNs of our proposed scheme during the broadcast phases can be written as

$$R_{\mathrm{Tx}}^{\mathrm{PU}_l}=\min\left\{C^*_{s_ld},C^*_{s_lr_k}\right\},\ \ l\in L\, k\in K. \tag{21}$$

As for the K RD links, each link obeys the adaptive modulation mode selection rule of (8) and (9). Additionally, the achievable rate of the CU/RN-to-BS link during the cooperative phases is given by

$$R_{\mathrm{Tx}}^{\mathrm{CU}_k}=\max\left\{C^*_{r_kd}\right\},\quad k\in K \tag{22}$$

where the values of $C^*_{s_ld}$, $C^*_{s_lr_k}$, and $C^*_{r_kd}$ can be obtained from (8), depending on the instantaneous channel conditions. Our proposed scenario achieves a FER lower than the 10^{-3} target at the RN, to minimize the potential error propagation from the CUs to the BS. The strategy defined in (21) during the broadcast phase is not the only scenario we have investigated. We have also tested another promising scenario, which select the best PU that has the highest SNR among all PUs, when the achievable rate is defined as $R_{\mathrm{Tx}}^{\mathrm{PU}_l}=\max\{C^*_{s_ld},C^*_{s_lr_k}\}$. However, the corresponding FER performance becomes worse than our target of 10^{-3}, which leads to an excessive probability of errors at the CUs. Hence, we ultimately recommend the better strategy of (21).

B. Analysis of Transmission Rate

Here, we investigate the attainable transmission rate of our proposed schemes. We assume that we have N-frame sessions, and the length of each TS in the frame is T. As discussed in Section II, this TS is split into two parts, yielding $T=T_1+T_2$, where T_1 is used for the PU's transmission during the broadcast phase, and T_2 is allocated for the CUs to relay the combined information of both the PU and CU during the cooperative phase. If the PU activates a higher throughput modulation mode, then the SNR required by the PU will be high. As a benefit, this will shorten the PU's transmission duration of T_1. Consequently, this would grant a longer transmission period for the CUs. Thus, we increase T_2, when T_1 is reduced. Moreover, we assumed that the PU and CU have the same Baud rate (symbol rate) of $R_s^{\mathrm{PU}}=R_s^{\mathrm{CU}}$ symbol/s during the entire transmission period. Meanwhile, the number of bits per frame of the PU and CU are the same, namely $N_b^{\mathrm{PU}}=N_b^{\mathrm{CU}}$ bits. Then, the number of bits during the broadcast phase is given by

$$N_b^{\mathrm{PU}}=\frac{LR_s^{\mathrm{PU}}}{R_{\mathrm{Tx}}^{\mathrm{PU}_l}} \tag{23}$$

whereas during the cooperative phase, it is

$$N_b^{\mathrm{CU}}=\frac{K'R_s^{\mathrm{CU}}}{R_{\mathrm{Tx}}^{\mathrm{CU}_k}} \tag{24}$$

where K' was defined in Section II-C2. Then, the Baud rate of the PU is $R_s^{\mathrm{PU}}=N_b^{\mathrm{PU}}/T_1$, whereas that of the CU is $R_s^{\mathrm{CU}}=N_b^{\mathrm{CU}}/T_2$.

In our proposed DNC-CCR scheme of Section II-B, the TSs are shared by the PU and CU. We assumed that the amount of information to be transmitted by the PU and CU is identical; thus, we have

$$\frac{LR_s^{\mathrm{PU}}}{R_{\mathrm{Tx}}^{\mathrm{PU}_l}T_1}=\frac{K'R_s^{\mathrm{CU}}}{R_{\mathrm{Tx}}^{\mathrm{CU}_k}T_2}. \tag{25}$$

Then, based on (25), the relationship between T_1 and T_2 is given by

$$\frac{T_2}{T_1}=\frac{K'R_{\mathrm{Tx}}^{\mathrm{PU}_l}}{LR_{\mathrm{Tx}}^{\mathrm{CU}_k}}. \tag{26}$$

Since $T_2=T-T_1$, based on (26), we have

$$T_1=\frac{LR_{\mathrm{Tx}}^{\mathrm{CU}_k}}{K'R_{\mathrm{Tx}}^{\mathrm{PU}_l}+LR_{\mathrm{Tx}}^{\mathrm{CU}_k}}T. \tag{27}$$

The average throughput of the entire system may be quantified by the ratio of the total number of transmitted information bits divided by the number of transmission TSs. This metric is similar to the concept of the overall rate defined in [27, (18)]. We also assume that our proposed system transmits its messages at the same rate during each N-frame session. Then, the overall throughput per frame per user for our proposed DNC-CCR scheme is given by

$$\eta_{\mathrm{DNC}}=\frac{1}{N}\sum_{n=1}^{N}\frac{\sum_{l=1}^{L}R_{\mathrm{Tx}}^{\mathrm{PU}_l}T_1}{L\times T} \tag{28}$$

$$=\frac{1}{N}\sum_{n=1}^{N}\frac{\sum_{l=1}^{L}\frac{LR_{\mathrm{Tx}}^{\mathrm{PU}_l}R_{\mathrm{Tx}}^{\mathrm{CU}_k}}{\left(K'R_{\mathrm{Tx}}^{\mathrm{PU}_l}+LR_{\mathrm{Tx}}^{\mathrm{CU}_k}\right)}}{L\times T} \tag{29}$$

where again N denotes the number of frames, and L is the total number of PUs. In our $M_{2\times 4}$-based system, the number of frames transmitted from the PU is $L \times m_1 = 2$, whereas the number of information frames transmitted from the PUs is $L \times m_1 = 4$ for the $M_{4\times 8}$-based system.

1) ADNC Scheme: Let us now consider the achievable transmission rate of our proposed ADNC-CCR scheme. If all the PUs transmit all their messages to the BS successfully, the CUs do not have to relay the source information to the BSs. By contrast, the CUs will relay the source information to the BS if the transmissions from the PU to the BS failed. Thus, we can obtain the time allocations between PUs and CUs as follows:

$$T_1 \begin{cases} = T, T_2 = 0, & \text{if the PU's transmission is successful.} \\ = \frac{L R_{\mathrm{Tx}}^{\mathrm{CU}_k}}{K' R_{\mathrm{Tx}}^{\mathrm{PU}_l} + L R_{\mathrm{Tx}}^{\mathrm{CU}_k}} T, T_2 = T - T_1, & \text{otherwise} \end{cases}$$

where K' is different in the ADNC-M1 scheme of Section II-C1 and in the ADNC-M2 scheme of Section II-C2. Moreover, if the PU transmitted successfully to the BS, we can save the entire T_2 duration for the CU's communication. However, if the PU failed to successfully transmit its message to the BS, then the CU would relay the PU's message to the BS. If the transmit SNR of the PU is higher, the relaying period of the CU will be reduced, and this allows the system to grant longer transmit duration for the CUs. By contrast, at a low SNR, the opposite trend prevails. When the PU's transmission is successful, the average throughput of L PUs relying on our ADNC-CCR scheme is given by

$$\eta_{\mathrm{ADNC}} = \frac{1}{N} \sum_{n=1}^{N} \frac{\sum_{l=1}^{L} R_{\mathrm{Tx}}^{\mathrm{PU}_l} T}{LT} = \frac{1}{N} \sum_{n=1}^{N} \frac{\sum_{l=1}^{L} R_{\mathrm{Tx}}^{\mathrm{PU}_l}}{L}. \tag{30}$$

If the PU's transmission failed, then the CU/RN will transmit the PU's information to the BS. The overall throughput takes into consideration both the PU's information and the CU's own information, where we have $\eta_{\mathrm{ADNC}} = \eta_{\mathrm{DNC}}$ when the PU's transmission failed; η_{DNC} is detailed in (29). Hence, the overall throughput per frame per user of the proposed ADNC scheme is given by

$$\eta_{\mathrm{ADNC}} = \begin{cases} \frac{1}{N} \sum_{n=1}^{N} \frac{\sum_{l=1}^{L} R_{\mathrm{Tx}}^{\mathrm{PU}_l}}{L}, & \text{PU's transmission was successful} \\ \frac{1}{N} \sum_{n=1}^{N} \frac{\sum_{l=1}^{L} R_{\mathrm{Tx}}^{\mathrm{PU}_l} T_1}{L \times T}, & \text{PU's transmission failed} \end{cases}$$

where T_1 is defined in (27).

2) Direct Transmission: The overall transmission rate per frame per user of the noncooperative scheme recorded for the whole TS duration T becomes

$$\eta_{\mathrm{sd}} = \frac{1}{N} \sum_{n=1}^{N} \frac{\sum_{l=1}^{L} R_{\mathrm{Tx}}^{\mathrm{PU}_l}}{L}. \tag{31}$$

Finally, we will compare the overall performance of these two systems in Section IV.

C. Diversity Order and Network Code Rate

The NC rate R_{NC} characterizing the multiplexing capability of the NC scheme exemplified in Section II-B may be expressed as

$$R_{\mathrm{NC}} = \frac{\text{Total number transmitted information frames of PUs}}{\text{Total number of information frames of PUs and CUs}}. \tag{32}$$

By further considering the ADNC scheme detailed in Section II-C, the network code rate of ADNC-M1 is given by

$$R_{\mathrm{NC}}^{\mathrm{ADNC-M1}} = \begin{cases} \frac{Lm_1}{Lm_1}, & S_f = 1 \\ \frac{Lm_1}{Lm_1 + Km_2}, & S_f = 0. \end{cases} \tag{33}$$

Moreover, the NC rate of the ADNC-M2 scheme may be expressed as

$$R_{\mathrm{NC}}^{\mathrm{ADNC-M2}} = \begin{cases} \frac{Lm_1}{Lm_1}, & \sum_l^L (S_{f_l}) = 1 \\ \frac{Lm_1}{Lm_1 + Km_2}, & \sum_l^L (S_{f_l}) = 0 \\ \frac{Lm_1}{Lm_1 + \vartheta m_2}, & \text{otherwise} \end{cases} \tag{34}$$

where the number of CUs is assumed the same as the number of PUs in our design. As shown in (33) and (34), the resultant NC rate is $R_{\mathrm{NC}}^{\mathrm{ADNC}} = (Lm_1/Lm_1) = 1$, whereas the value of Km_2 can be adaptively adjusted toward zero to increase the achievable multiplexing gain. To highlight our generic design principles, the $M_{4\times 8}$-based system is taken into consideration. The transfer matrix $M_{4\times 8}$ is provided by [16], [17]:

$$M_{4\times 8} = \left[\begin{array}{cccc|cccc} 1 & 0 & 0 & 0 & 3 & 7 & 3 & 6 \\ 0 & 1 & 0 & 0 & 5 & 7 & 7 & 4 \\ 0 & 0 & 1 & 0 & 2 & 4 & 6 & 1 \\ 0 & 0 & 0 & 1 & 5 & 5 & 3 & 2 \end{array}\right]. \tag{35}$$

Then, we have four broadcast phases and four cooperative phases. The construction of the parity frames P_k of the kth CU is detailed in (13). Moreover, the modified transfer matrix M' of the actual communication is given by $M'_{4\times 8}(i,j) = M_{4\times 8}(i,j)$, provided that all transmitted frames are successfully decoded by the BS. Referring to Fig. 1, the network encoders of the CUs generate the parity frames based on the information frames. The network decoders at the BS will decode the parity frames based on the modified matrix introduced in Section II-B. Therefore, the $M_{2\times 4}$-based scheme and the $M_{4\times 8}$-based scheme are comparable since they share the same parameter values of $R_{\mathrm{NC}}^{\mathrm{ADNC}} = (Lm_1/(Lm_1 + Km_2)) = 1/2$, whereas $S_f = 0$ or $\sum_l^L (S_{f_l}) = 0$ refer to (33) and (34), respectively.

Accordingly, the information rate R_{info} of our proposed system can be expressed as [17]

$$R_{\mathrm{info}} = R_{\mathrm{NC}} \times \eta_{\mathrm{ADNC}} \tag{36}$$

which is near-instantaneously time variant [37], [38] since it may be changed for each transmission session. Furthermore, the diversity order reflecting the degree of space diversity gain attained by employing our NC-aided system may be expressed as [39]

$$D_{\mathrm{ADNC}} = K' + m_2 \tag{37}$$

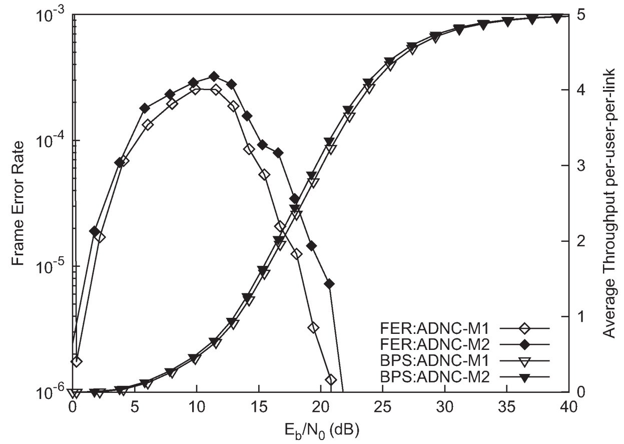

Fig. 5. FER performance and average throughput per user per link versus Eb/N_0 of the proposed ATTCM-aided ADNC scheme based on the $M_{4\times8}$ matrix detailed in Section III, as well as of ADNC-M1 for $K' \in 0, 4$, and ADNC-M2 for $K' \in 0, 1, 2, 3, 4$.

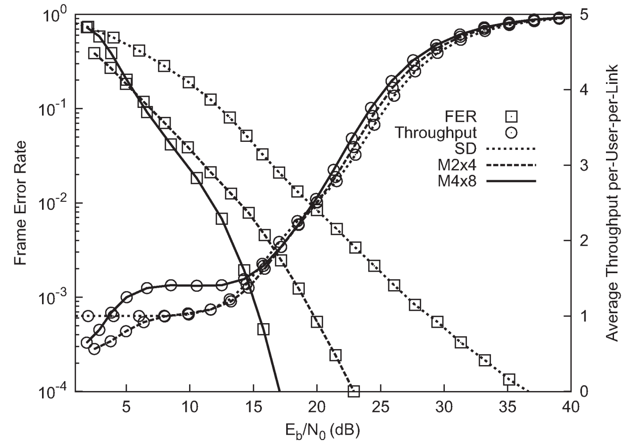

Fig. 6. FER performance and average throughput per user per link versus $Eb/N0_t$ of the proposed System 2 of the ATTCM-aided ADNC scheme; see Table I. "M2x4" and "M4x8" represent the FER and average throughput of our ATTCM-aided ADNC scheme activating one of the five channel-quality-dependent modulation modes using 10^6 frames based on the matrix $M_{2\times4}$ and $M_{4\times8}$, respectively.

where the value of K' is $K' \in [0, 4]$ for the ADNC-M1 scheme and $K' \in [0, 1, 2, 3, 4]$ for the ADNC-M2 scheme, when $M_{4\times8}$ is used. In addition, the maximum and minimum values of $D_{\mathrm{ADNC-M1}}$ are identical to those of $D_{\mathrm{ADNC-M2}}$, but the diversity order $D_{\mathrm{ADNC-M1}}$ is higher than in the scenario $D_{\mathrm{ADNC-M2}}$, when the BS fails to recover the PU's information since the value of K' in the $D_{\mathrm{ADNC-M2}}$ scheme can be [1, 2, 3]. Fig. 5 shows both the FER performance and the average per-user per-link throughput versus E_b/N_0 for our ATTCM-aided ADNC assisted CCR system based on the $M_{4\times8}$ matrix. It is shown in Fig. 5 that the FER performance of ADNC-M1 is better than that of the ADNC-M2 since it has a higher diversity order in some situations, when their throughputs are comparable. In our CCR scheme, we aim for reducing the bandwidth requirement, while increasing the transmission rate of the PUs. We will employ ANDC-M2 in the investigations of Section IV because it has a higher multiplexing gain.

IV. Numerical Results and Discussions

Fig. 2 shows the FER performance of the five individual nonadaptive TTCM modes of (8), when communicating over uncorrelated Rayleigh fading channels and the FER of TTCM-aided DNC and of the corresponding noncooperative schemes, when transmitting over our combined[1] quasi-static (shadow) and Rayleigh (fast) fading channels. Fig. 2 substantiates that the curves that consider only an uncorrelated Rayleigh fading channel always exhibit a better performance than the curves that characterize the combined quasi-static and Rayleigh fading scenarios. It is observed that the FER performance of our ATTCM-aided DNC scheme is always better than that of the noncooperative scheme, regardless of the specific modulation modes. Naturally, the 4PSK modulation mode has the best FER performance. It is shown in Fig. 2 that the DNC-4PSK arrangement attains an approximately 20 dB gain, in comparison to the SD-4PSK scheme at FER $= 10^{-3}$. As expected, the 64QAM mode has the worst FER performance. When viewing this comparison for an SNR perspective, the DNC-64QAM scheme required an extra 12 dB power compared with both DNC-4PSK and to DNC-64QAM.

We define E_b/N_0 as the ratio of transmitted energy per bit to-noise power spectral density, i.e.,

$$E_b/N_0 \text{ dB} = \gamma_t \text{ dB} - 10\log_{10}(R_{\mathrm{info}}) \tag{38}$$

where γ_t is the *transmit SNR*[2], and R_{info} is the system's achievable throughput, which is defined in (36).

Fig. 6 shows the FER versus E_b/N_0 performance of the $M_{2\times4}$ and $M_{4\times8}$-based System 2 employing the ADNC arrangement, which represents the practical ATTCM transmission scheme of Table I, as introduced in Section II-A. Its performance is benchmarked against that of the ATTCM-aided noncooperative communication scheme. As observed in Fig. 6, the $M_{4\times8}$-based scheme is capable of providing a significant E_b/N_0 performance improvement of $19 - 15 = 4$ dB at FER $=10^{-3}$ in comparison to the $M_{2\times4}$-based scheme. In comparison to the noncooperative schemes, our proposed $M_{4\times8}$ and $M_{2\times4}$-based ADNC arrangement has a better FER performance. More specifically, our $M_{4\times8}$-based scheme attains an approximately $27 - 15 = 8$ dB gain compared with its noncooperative counterpart at FER $= 10^{-3}$.

As discussed in Section III-B, the average throughput per user of the entire system can be summarized as

$$\bar{\eta}_{\mathrm{ave}} = \frac{\overbrace{LR^{\mathrm{PU}}_{\mathrm{tran}}T_{\mathrm{broadcast}}}^{\text{Transmitted packet of PU}}}{\underbrace{LT_{\mathrm{broadcast}} + KT_{cooperative}}_{\text{Required orthogonal channel}}} = \frac{LR^{\mathrm{PU}}_{\mathrm{tran}}}{L+K}. \tag{39}$$

[1]When the channel gain incorporates both the shadow-fading and fast-fading components, the adaptive transmission regime counteracts the shadow fading, but it is typically unable to accommodate the Rayleigh fading.

[2]The concept of transmit SNR [32] is unconventional, as it relates quantities to each other at two physically different locations, namely, the transmit power to the noise power at the receiver, which are at physically different locations. However, this is a computationally convenient definition.

TABLE I
MAIN PARAMETERS OF OUR TWO SYSTEMS, WHERE SYSTEM 1 INCLUDES A NO TRANSMISSION MODE, WHEREAS SYSTEM 2 WOULD INVOKE THE "TTCM-4PSK" MODE WHEN THE CHANNEL QUALITY IS POOR

System	System 1	System 2
The output $C^*(\gamma_R < \gamma_0)$	case 1 (No transmission)	case 2 (TTCM-4PSK)
Principle of ADNC	ADNC-M2	ADNC-M2
Channel	Rayleigh and Quasi static fading channel	Rayleigh and Quasi static fading channel
Number of frames N	10^6	10^6
Adaptive Coding	ATTCM	ATTCM
Modulation	Q-PSK, 8-PSK, 16-QAM, 32-QAM, 64-QAM	Q-PSK, 8-PSK, 16-QAM, 32-QAM, 64-QAM
FER bound	10^{-3}	10^{-3}
Transfer matrix of DNC	$M_{2\times4}$, $M_{4\times8}$	$M_{2\times4}$, $M_{4\times8}$
Number of PUs	$L = 2, 4$	$L = 2, 4$
Number of CUs	$K = 2, 4$	$K = 2, 4$
m_1 [frame]	1	1
m_2 [frame]	1	1
Pathloss exponent α	3	3

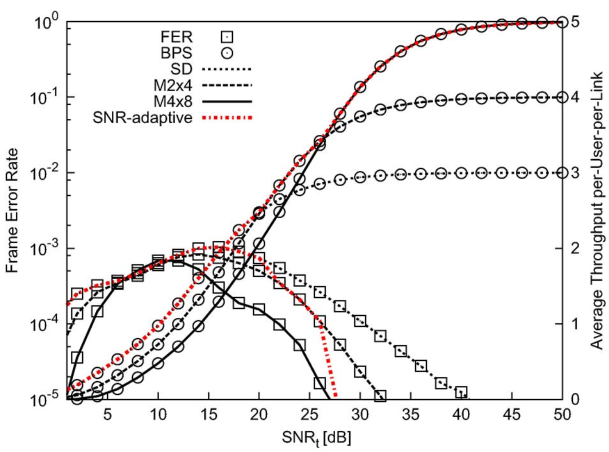

Fig. 7. FER performance and average throughput per user per link versus SNR$_t$ of the proposed System 1 of the ATTCM-aided ADNC scheme; see Table I. "SD," "M2x4," and "M4x8" represent the FER and average throughput of our ATTCM-aided noncooperative scheme using one of three modulation modes and the ADNC scheme for four and five modulation modes based on matrices $M_{2\times4}$ and $M_{4\times8}$. "SNR-adaptive" ATTCM-ADNC-CCR scheme is represented to be the scheme always activates the best scheme for the set of "SD"-, "M2x4"-, and "M4x8"-based schemes in terms of the average throughput as a function of the SNR, which is described in Section IV. The number of transmitted frames is 10^6.

Explicitly, Fig. 6 shows the average throughput per user per link versus E_b/N_0 performance of the $M_{2\times4}$ and $M_{4\times8}$-based ATTCM-ADNC-CCR scheme, when we employed the five TTCM modes of (8) and used the case 2 scenario of (9). In contrast to the ADNC arrangement, at low SNRs, the noncooperative arrangement has a throughput of 1 iBPS. It is observed in Fig. 6 that the throughput trends of these three schemes are similar, and they approach 5 iBPS at $E_b/N_0 =$ 40 dB. Therefore, the $M_{4\times8}$-based scheme has the best FER performance at a comparable throughput.

Fig. 7 shows the FER versus SNR$_t$ performance of $M_{2\times4}$ and $M_{4\times8}$-based System 1 employing the ADNC arrangement; the parameters are shown in Table I. In Fig. 7, we compare the throughput of three schemes at a comparable FER. Explicitly, the noncooperative scheme employed the BPSK, 8PSK, and 16QAM of ATTCM transmission modes. The reason for considering three modulation modes for our noncooperative scheme is because the FER performance of the noncooperative benchmark scheme is somewhat poor. If a 32QAM modulation mode were to be used, the FER would become excessive. Hence, we opted for four modulation modes for our ATTCM-ADNC-CCR $M_{2\times4}$ matrix. Observe in Fig. 7 that the FER recorded at the RN becomes lower than 10^{-3} both for the ADNC and for the noncooperative scheme. The FER performance curves of the $M_{2\times4}$ and $M_{4\times8}$-based ATTCM-ADNC-CCR schemes and of the noncooperative scheme crossed each other at SNR$_t = 10$ dB. Beyond that point, the FER performance of the ADNC scheme became better than that of the noncooperative scheme, namely for SNR$_t > 11$ dB. Moreover, at FER $= 10^{-5}$, our proposed $M_{4\times8}$-based scheme attains a $40 - 26.5 = 13.5$ dB gain compared with the noncooperative scheme.

As observed in Fig. 7, our proposed $M_{4\times8}$-based ADNC scheme has a better throughput than the noncooperative scheme for SNR$_t > 25$ dB. Explicitly, we found in Fig. 7 that the ADNC scheme achieved a throughput of 5.0 iBPS, which is $5.0 - 3.0 = 2.0$ bits higher than that of the noncooperative scheme at SNR$_t = 45$ dB. Observe furthermore in Fig. 7 that the throughput of the $M_{2\times4}$-based ADNC scheme is higher than that of the noncooperative scheme for SNR$_t > 20$ dB. More specifically, the proposed $M_{4\times8}$-based ADNC scheme requires four TSs, whereas the $M_{2\times4}$-based scheme only requires two TSs when the BS failed to flawlessly receive the source information from the SN, albeit these ADNC schemes failed to achieve a higher throughput for low SNR$_t$. Hence, it is better to activate a noncooperative model at a low SNR since its throughput per user per link is better. Then, the "SNR-adaptive" ATTCM-ADNC-CCR system characterized in Fig. 7 is the scheme that always activates the best scheme for the set of noncooperative $M_{2\times4}$-based and $M_{4\times8}$-based systems in terms of the average throughput as a function of the SNR. Note that, at FER $= 10^{-4}$ the FER performance of the "SNR adaptive" scheme is better than that of the $M_{2\times4}$-based arrangement, but at FER $= 10^{-5}$, it is worse than that of the $M_{4\times8}$-based scheme.

The bandwidth-reduction factor B_s may be formulated as [20]

$$B_s = 1 - \frac{\eta_{\rm sd}}{\bar{\eta}_{\rm ave}} \tag{40}$$

where $\eta_{\rm sd}$ denotes the throughput of the noncooperative system employing ATTCM as defined in (31), and $\bar{\eta}_{\rm ave}$ is defined in (39).

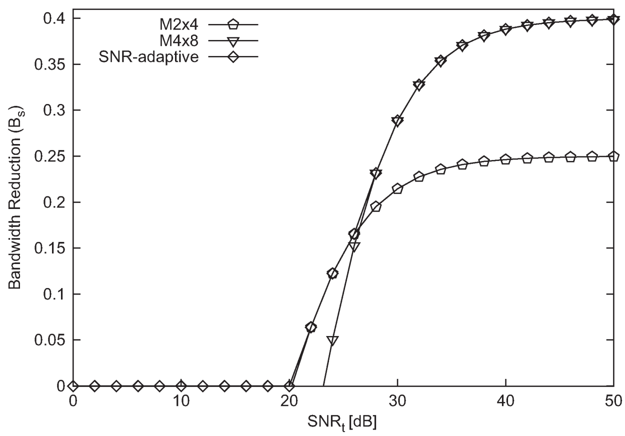

Fig. 8. Bandwidth reduction B_s versus SNR_t of the proposed System 1 of ATTCM-aided ADNC scheme; see Table. I. "SD," "M2x4," and "M4x8" denote the FER and average throughput of ATTCM-aided noncooperative scheme using one of three modulation modes and the ADNC scheme for four and five modulation modes based on matrices $M_{2\times4}$ and $M_{4\times8}$. The "SNR-adaptive" ATTCM-ADNC-CCR scheme is represented to be the scheme that always activates the best scheme for the set of "SD"-, "M2x4"-, and "M4x8"-based schemes in terms of the average throughput as a function of the SNR, which is described in Section IV.

In Fig. 8, we consider the attainable bandwidth reduction versus SNR_t for our ATTCM-ADNC-CCR system based on the $M_{2\times4}$ and $M_{4\times8}$ matrices of Table I. It is observed in Fig. 8 that the highest bandwidth reduction is achieved by the $M_{4\times8}$-based ADNC scheme, which result in $B_s = 40\%$ for $\mathrm{SNR}_t \geq 42$ dB. Observe in Fig. 7 that the corresponding maximum throughput of the ADNC scheme is $\eta_{\mathrm{ADNC}} = 5$, whereas that of the noncooperative scheme is $\eta_{\mathrm{sd}} = 3$. Thus, based on (40), we arrive at $B_s = 1 - (3/5) = 0.4 = 40\%$. By referring to Fig. 8, we observe that the $M_{2\times4}$-based scheme may achieve $B_s = 25\%$ at high SNRs, namely for $\mathrm{SNR}_t \geq 42$ dB. Thus, the $M_{4\times8}$-based ADNC scheme is capable of saving $40\% - 25\% = 15\%$ more bandwidth than the $M_{2\times4}$-based ADNC scheme. Moreover, the performance of the "SNR-adaptive" ATTCM-ADNC-CCR scheme characterized in Fig. 8 provides the highest bandwidth for the PU, regardless of the SNR. In our proposed ADNC-CCR schemes, the size of the DNC matrix and the number of frames transmitted per PU/CU would influence the number of supported PUs. More specifically, based on a $(N_r \times N_c)$-element DNC matrix $M_{N_r\times N_c}$, the number of PUs that can be supported over an N_r-frame periods is given by N_r/N_f, where N_f is the number of frames transmitted per PU during the N_r-frame period. Hence, the $M_{4\times8}$-based DNC-CCR scheme is capable of supporting $L = \{1, 2, 4\}$ PUs when we have $N_f = \{4, 2, 1\}$, respectively. We found that both the FER and the average throughput per user per link versus SNR_t performance would be similar, when supporting various number of PUs when using the same transfer matrix. Investigations based on a larger DNC matrix, such as the $M_{6\times12}$ of [40], will be considered in our future work.

V. Conclusion

An ATTCM-aided ADNC-assisted CCR scheme was conceived, where both the ATTCM modulation mode and the ADNC technique were configured according to the near-instantaneous channel conditions. We found that the proposed ADNC-aided CCR scheme enables the PU to either transmit 2 iBPS more information at a given SNR or releasing up to 40% of bandwidth for exploitation by the CUs.

References

[1] F. K. Jondral, "Cognitive radio: A communications engineering view," *IEEE, Wireless Commun.*, vol. 14, no. 4, pp. 28–33, Aug. 2007.

[2] J. Mitola and G. Q. Maguire, "Cognitive radio: Making software radios more personal," *IEEE Pers. Commun.*, vol. 6, no. 4, pp. 13–18, Aug. 1999.

[3] N. Devroye, P. Mitran, and V. Tarokh, "Achievable rates in cognitive radio channels," *IEEE Trans., Inf. Theory*, vol. 52, vol. 52, no. 5, pp. 1813–1827, May 2006.

[4] B. Wang and K. Liu, "Advances in cognitive radio networks: A survey," *IEEE J. Sel. Topics Signal Process.*, vol. 5, no. 1, pp. 5–23, Feb. 2011.

[5] A. Goldsmith, S. Jafar, I. Maric, and S. Srinivasa, "Breaking spectrum gridlock with cognitive radios: An information theoretic perspective," in *Proc. IEEE*, vol. 97, no. 5, pp. 894–914, May 2009.

[6] K. B. Letaief and W. Zhang, "Cooperative communications for cognitive radio networks," *Proc. IEEE*, vol. 97, no. 5, pp. 878–893, May 2009.

[7] Y. Li, "Distributed coding for cooperative wireless networks: An overview and recent advances," *IEEE Commun. Mag.*, vol. 47, no. 8, pp. 71–77, Aug. 2009.

[8] K. Loa *et al.*, "IMT-advanced relay standards [WiMAX/LTE Update]," *IEEE Commun. Mag.*, vol. 48, no. 8, pp. 40–48, Aug. 2010.

[9] D. Hwang, J. Choi, B. Clerckx, and G. Kim, "Mimo precoder selections in decode-forward relay networks with finite feedback," *IEEE Trans. Commun.*, vol. 59, no. 7, pp. 1785–1790, Jul. 2011.

[10] Z. Ding, K. Leung, D. Goeckel, and D. Towsley, "Opportunistic relaying for secrecy communications: Cooperative jamming vs. relay chatting," *IEEE Trans. Wireless Commun.*, vol. 10, no. 6, pp. 1725–1729, Jun. 2011.

[11] T. Korakis, M. Knox, E. Erkip, and S. Panwar, "Cooperative network implementation using open-source platforms," *IEEE Commun. Mag.*, vol. 47, no. 2, pp. 134–141, Feb. 2009.

[12] L. Chen, R. Carrasco, and I. Wassell, "Opportunistic nonorthogonal amplify-and-forward cooperative communications," *Electron. Lett.*, vol. 47, no. 10, pp. 626–628, Dec. 2011.

[13] M. Yassaee and M. Aref, "Slepian Wolf coding over cooperative relay networks," *IEEE Trans. Inf. Theory*, vol. 57, no. 6, pp. 3462–3482, Jun. 2011.

[14] F. Tian, W. Zhang, W.-K. Ma, P. Ching, and H. Poor, "An effective distributed space-time code for two-path successive relay network," *IEEE Trans. Commun.*, vol. 59, no. 8, pp. 2254–2263, Aug. 2011.

[15] M. Xiao and M. Skoglund, "Multiple-user cooperative communications based on linear network coding," *IEEE Trans. Commun.*, vol. 58, no. 12, pp. 3345–3351, Dec. 2010.

[16] J. Rebelatto, B. Uchoa-Filho, Y. Li, and B. Vucetic, "Adaptive distributed network-channel coding," *IEEE Trans. Wireless Commun.*, vol. 10, no. 9, pp. 2818–2822, Sep. 2011.

[17] J. Rebelatto, B. Uchoa-Filho, Y. Li, and B. Vucetic, "Multiuser cooperative diversity through network coding based on classical coding theory," *IEEE Trans. Signal Process.*, vol. 60, no. 2, pp. 916–926, Feb. 2012.

[18] M. Xiao, J. Kliewer, and M. Skoglund, "Design of network codes for multiple-user multiple-relay wireless networks," *IEEE Trans. Commun.*, vol. 60, no. 12, pp. 3755–3766, Jun./Jul. 2012.

[19] W. Liang, S. X. Ng and L. Hanzo, "Adaptive turbo trellis coded modulation aided cooperative cognitive radio," in *Proc. IEEE WCNC*, Apr. 2012, pp. 2362–2366.

[20] W. Liang, S. X. Ng, and L. Hanzo, "Cooperative communication between cognitive and primary users," *IET Commun.*, vol. 7, no. 17, pp. 1982–1992, 2013.

[21] R. Ahlswede, N. Cai, S.-Y. Li, and R. Yeung, "Network information flow," *IEEE Trans. Inf. Theory*, vol. 46, no. 4, pp. 1204–1216, Jul. 2000.

[22] R. Yeung, "Network coding: A historical perspective," *Proc. IEEE*, vol. 99, no. 3, pp. 366–371, Mar. 2011.

[23] S.-Y. Li, Q. Sun, and Z. Shao, "Linear network coding: Theory and algorithms," in *Proc. IEEE*, vol. 99, no. 3, pp. 372–387, Mar. 2011.

[24] X. Zhang, A. Ghrayeb, and M. Hasna, "On relay assignment in network-coded cooperative systems," *IEEE Trans. Wireless Commun.*, vol. 10, no. 3, pp. 868–876, Mar. 2011.

[25] X. Li, T. Jiang, S. Cui, J. An, and Q. Zhang, "Cooperative communications based on rateless network coding in distributed MIMO systems [coordinated and distributed MIMO]," *IEEE Wireless Commun.*, vol. 17, no. 3, pp. 60–67, Jun. 2010.
[26] S. Sharma *et al.*, "Network coding in cooperative communications: Friend or Foe?" *IEEE Trans. Mobile Comput.*, vol. 11, no. 7, pp. 1073–1085, Jul. 2012.
[27] L. Li, L. Wang, and L. Hanzo, "Generalized adaptive network coding aided successive relaying for noncoherent cooperation," *IEEE Trans. Commun.*, vol. 61, no. 5, pp. 1750–1763, May 2013.
[28] S. Wang, Y. Sagduyu, J. Zhang, and J. H. Li, "Spectrum shaping via network coding in cognitive radio networks," in *Proc. IEEE INFOCOM*, 2011, pp. 396–400.
[29] L. Hanzo, T. H. Liew, B. L. Yeap, R. Y. S. Tee, and S. X. Ng, *Turbo Coding, Turbo Equalisation and Space-Time Coding (EXIT-Chart-Aided Near-Capacity Designs for Wireless Channels)*. New York, NY, USA: Wiley, 2011.
[30] S. X. Ng, O. Alamri, Y. Li, J. Kliewer, and L. Hanzo, "Near-capacity turbo trellis coded modulation design based on EXIT charts and union bounds," *IEEE Trans. Commun.*, vol. 56, no. 12, pp. 2030–2039, Dec. 2008.
[31] L. Kong, S. X. Ng, R. Maunder, and L. Hanzo, "Maximum-throughput irregular distributed space-time code for near-capacity cooperative communications," *IEEE Trans. Veh. Technol.*, vol. 59, no. 3, pp. 1511–1517, Mar. 2010.
[32] H. Ochiai, P. Mitran, and V. Tarokh, "Design and analysis of collaborative diversity protocols for wireless sensor networks," in *Proc. IEEE 60th, VTC—Fall*, Sep. 2004, vol. 7, pp. 4645–4649.
[33] A. Tobagi Fouad and M. M. Hira, "Joint optimization of physical layer parameters and routing in wireless mesh networks," in *Proc. 9th IFIP Annu. Med-Hoc-Net*, Jun. 2010, pp. 1–8.
[34] L. Hanzo, S. X. Ng, T. Keller, and W. Webb, *Quadrature Amplitude Modulation:From Basics to Adaptive Trellis-Coded, Turbo-Equalised and Space-Time Coded OFDM, CDMA and MC-CDMA Systems*. Hoboken, NJ, USA: Wiley-IEEE Press, 2004.
[35] G. Ungerböck, "Channel coding with multilevel/phase signals," *IEEE Trans. Inf. Theory*, vol. IT-28, no. 1, pp. 55–67, Jan. 1982.
[36] SAGE, Open source mathematics software. [Online]. Available: http://www.sagemath.org/
[37] C. W. L. Hanzo and M. Yee, *Adaptive Wireless Transceivers: Turbo-Coded, Turbo-Equalized and Space-Time Coded TDMA, CDMA and OFDM Systems*. New York, NY, USA: Wiley, 2002.
[38] L. Hanzo, L. L. Yang, E. L. Kuan, and K. Yen, *Single- and Multi-Carrier DS-CDMA: Multi-User Detection, Space-Time Spreading, Synchronisation, Networking and Standards*. New York, NY, USA: Wiley, 2003.
[39] H. V. Nguyen *et al.*, "Network coded MIMO aided cooperative communications in the ambulance-and-emergency area," in *Proc. MoWNet*, 2014, pp. 214–221.
[40] H. V. Nguyen, S. X. Ng, and L. Hanzo, "Irregular convolution and unity-rate coded network coding for cooperative multi-user communications," *IEEE Trans. Wireless Commun.*, vol. 12, no. 3, pp. 1231–1243, Mar. 2013.

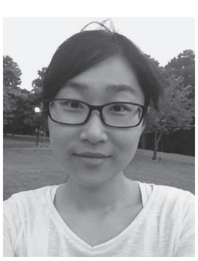

Wei Liang received the M.Sc. degree in wireless communications from the University of Southampton, Southampton, U.K., in 2010. She is currently working toward the Ph.D. degree with the Southampton Wireless Group, School of Electronics and Computer Science, University of Southampton.

Her current research interests include adaptive coded modulation, network coding, cooperative communications, and cognitive radio networks.

Hung Viet Nguyen received the B.Eng. degree in electronics and telecommunications from Hanoi University of Science and Technology, Hanoi, Vietnam, in 1999; the M.Eng. degree in telecommunications from the Asian Institute of Technology, Bangkok, Thailand, in 2002 and the Ph.D. degree in wireless communications from the University of Southampton, Southampton, U.K., in 2013.

Since 1999, he has been a Lecturer with the Post and Telecommunications Institute of Technology, Hanoi. He is currently a Postdoctoral Researcher with Southampton Wireless Group, School of Electronics and Computer Science, University of Southampton. His research interests include cooperative communications, channel coding, network coding, and quantum communications.

Soon Xin Ng (S'99–M'03–SM'08) received the B.Eng. degree (first class) in electronic engineering and the Ph.D. degree in telecommunications from the University of Southampton, Southampton, U.K., in 1999 and 2002, respectively.

From 2003 to 2006, he was a Postdoctoral Research Fellow, working on collaborative European research projects known as SCOUT, NEWCOM, and PHOENIX. Since August 2006, he has been a member of academic staff with the School of Electronics and Computer Science, University of Southampton. He is involved in the OPTIMIX and CONCERTO European projects and the IU-ATC and UC4G projects. He is currently an Associate Professor in telecommunications with the University of Southampton. He is the author of over 180 papers and the coauthor of two John Wiley/IEEE Press books in this field. His research interests include adaptive coded modulation, coded modulation, channel coding, space–time coding, joint source and channel coding, iterative detection, orthogonal frequency-division multiplexing, multiple-input–multiple-output systems, cooperative communications, distributed coding, quantum error correction codes, and joint wireless-and-optical-fiber communications.

Dr. Ng is a Fellow of the Higher Education Academy in the U.K. and is a Chartered Engineer.

Lajos Hanzo (M'91–SM'92–F'04) received the Master's degree in electronics, the Ph.D. degree, and the *Doctor Honoris Causa* degree from the Technical University of Budapest, Budapest, Hungary, in 1976, 1983, and 2009, respectively, and the D.Sc. degree from the University of Southampton, Southampton, U.K., in 2004.

During his career in telecommunications, he has held various research and academic posts in Hungary, Germany, and the U.K. Since 1986, he has been with the School of Electronics and Computer Science, University of Southampton, Southampton, U.K., where he holds the Chair in telecommunications. He was a Chaired Professor of Tsinghua University, Beijing, China. He is the coauthor of 20 John Wiley/IEEE Press books on mobile radio communications, totalling in excess of 10 000 pages, and has published more than 1400 research entries on IEEE Xplore. He is currently directing an academic research team, working on a range of research projects in the field of wireless multimedia communications sponsored by industry, the Engineering and Physical Sciences Research Council (EPSRC) U.K., the European IST Program, and the Mobile Virtual Centre of Excellence, U.K. He is an enthusiastic supporter of industrial and academic liaison, and he offers a wide range of industrial courses.

Dr. Hanzo has acted as a Technical Program Committee Chair for IEEE conferences, presented keynote lectures, and has received a number of distinctions. He is the Governor of the IEEE Vehicular Technology Society and the Past Editor-in-Chief of the IEEE Press.